Int J Clin Exp Med 2016;9(10):18946-18961
www.ijcem.com /ISSN:1940-5901/IJCEM0031926

Original Article

Potential serum microRNA signatures of pediatric IgA nephropathy

Qiang Sun[1,2], Xiaorong Liu[1,2], Nan Zhou[1,2], Hong Zhang[1,2], Ying Shen[1,2]

[1]Department of Nephrology, Beijing Children's Hospital, Capital Medical University, No. 56, Nanlishi Road, West District, Beijing 100045, China; [2]Beijing Key Laboratory of Pediatric Chronic Kidney Disease and Blood Purification, No. 56, Nanlishi Road, West District, Beijing 100045, China

Received May 9, 2016; Accepted August 13, 2016; Epub October 15, 2016; Published October 30, 2016

Abstract: IgA nephropathy (IgAN) is one of the most common causes leading to end-stage renal failure. The regulatory mechanisms underlying the emergence of microRNA are poorly understood and need to be studied for developing better strategies for diagnosis and treatment of pediatric IgA nephropathy. We performed a microRNA sequence analysis of the plasma microRNAs of pediatric patients with IgA nephropathy and healthy control by next generation sequencing (NGS) using the Illumina Deep Sequencing technology. We obtained 18,395,453, 11,348,541 and 22,646,434 qualified Illumina reads from three healthy controls, or 4,287,101, 5,473,799, 5,598,305, 7,713,565, 3,766,914, 7,249,629, 4,199,660, 5,623,320 and 3,014,665 qualified Illumina reads from nine pediatric patients, respectively. Comparative microRNAs analysis differentially revealed 2591 microRNAs between pediatric patients and healthy controls, one expression of microRNA was up-regulated and 19 expressions of microRNA were down-regulated. The volcano plot was used to further identify differential microRNAs expression between the two groups. Cluster analysis was performed, and spearman correlation coefficient was calculated and analyzed. Gene ontology (GO) consortium and data were used to analyze the targets gene of different microRNAs. Our work demonstrated differential microRNAs between pediatric patients and healthy controls. Numbers of microRNAs will serve as a promising resource for revealing the regulatory molecular mechanisms of expression associated with the pathophysiology and pathogenesis of IgAN, even their implications in the field of therapy.

Keywords: MicroRNA, IgA nephropathy (IgAN), next generation sequencing (NGS)

Introduction

IgA nephropathy (IgAN) is a common primary glomerular disease with 20-30% leading to end stage renal failure requiring long-term and regular dialysis or renal transplantation [1, 2]. IgAN is characterized by mesangial IgA-containing immune deposits, often with IgG and/or IgM co-deposits [3, 4]. However, the pathogenesis of IgAN is not clear, and may be related to genetics, immunology, environment, as well as other factors. The research regarding the pathogenesis of IgAN will benefit the diagnosis, treatment and prevention of the illness, and ultimately improve patient's prognosis and quality of life.

MicroRNAs (miRNAs) are an approximately 22 nucleotides (nt) long subset of non-coding RNAs, and can base pair with target messenger RNAs (mRNAs) to exert post-transcriptional regulation of gene expression. In the nucleus miRNAs are transcribed as pri-miRNAs, then processed to pre-miRNAs and finally transfered to cytoplasm with a 22 nts mature duplex. Combined with the RNA-induced silencing complex (RISC), one strand of miRNA interacts with its target mRNA usually binding within 3' untranslated regions (UTRs) via base-pairing, meanwhile the other can often be degraded [5]. With regard to the complementarity level of miRNA-mRNA, the translation of target mRNA can be repressed or degraded [6].

MiRNAs are released by cells into the bodily fluids (i.e. plasma, serum, urine etc.) and exist in kinds of cells and tissues. Their involvement occurs in three different ways: (i) dysregulation of miRNA levels; (ii) a genetic variant of miRNA that alters the binding; and (iii) alteration within

Table 1. The capacity of sequencing

Sample	Read (#)	Data (bp)
Control 1 (14001)	18,395,453	385,693,105
Control 2 (14002)	11,348,541	242,670,299
Control 3 (14003)	22,646,434	470,734,166
Patient 1 (XH)	4,287,101	154,335,636
Patient 2 (LXY)	5,473,799	197,056,764
Patient 3 (XMX)	5,598,305	201,538,980
Patient 4 (LZD)	7,713,565	277,688,340
Patient 5 (ZMY)	3,766,914	135,608,904
Patient 6 (MCW)	7,249,629	260,986,644
Patient 7 (ZWH)	4,199,660	151,187,760
Patient 8 (WYH)	5,623,320	202,439,520
Patient 9 (LTJ)	3,014,665	108,527,940

Table 2. The quality of sequencing

Sample	Q20 (%)	Q30 (%)
Control 1 (14001)	99.18	97.51
Control 2 (14002)	99.64	98.14
Control 3 (14003)	99.42	97.43
Patient 1 (XH)	99.17	97.51
Patient 2 (LXY)	99.20	97.73
Patient 3 (XMX)	99.52	98.19
Patient 4 (LZD)	99.17	97.55
Patient 5 (ZMY)	99.09	97.41
Patient 6 (MCW)	99.16	97.55
Patient 7 (ZWH)	99.31	97.82
Patient 8 (WYH)	99.53	98.20
Patient 9 (LTJ)	99.55	98.24

3'-UTRs of mRNA. MiRNAs are relatively stable. Being contained in circulating vesicles or carried by circulating the Argonauts 2 complex account for the stability of circulating miRNAs [7].

Serum, plasma and PBMCs (peripheral blood mononuclear cells) contain plenty of miRNAs; studies have demonstrated that they make up a pool of candidate molecules forming specific classifiers for diagnosis of diseases and monitoring their outcomes. MiRNAs have been selected on the basis of their fold changes and potential value in the pathogenesis of disease. For this reason, miRNAs may be considered as strategic candidate biomarkers for non-invasive diagnosis and early detection of disease. In the last 5 years, evidence has demonstrated that miRNAs were involved in the development of kidney and essential for normal renal function [8-11]. A cluster of miRNAs have been identified in the human kidney such as miR-192, miR-194, miR-204 and miR-215 [12] and a differential profile of miRNA expression has been shown in the renal cortex and medulla of rat kidney [13]. MiRNAs in the development and progression of renal damage can be considered as potential therapeutic targets in kidney diseases. Moreover, how miRNA mediates mRNA expression regulation at translation level in pediatric patients with IgAN remains unclear. This present study is to highlight the role of miRNAs in the pathophysiology and pathogenesis of IgAN.

Materials and methods

Patients and specimens

IgAN group: The study consisted of nine children diagnosed with primary IgAN. Inclusion criteria: (1) 18 year old or below; (2) children with primary IgAN; (3) confirmed by renal biopsy; (4) proteinuria and/or hematuria; (5) informed consent; (6) before immunosuppressive therapy; (7) without acute infection last month; (8) without cardiopulmonary or other diseases.

Healthy control group: Three healthy children with normal routine urinalysis were included.

All included patients and healthy children were referred to Beijing Children's Hospital, Capital Medical University from 2011 to 2015. At the next day of renal biopsy, anticoagulant blood was collected and handled immediately.

This study and use of human specimens in this research were approved by the Ethics Committee of Beijing Children's Hospital, Capital Medical University on the basis of the Declaration of Helsinki. We clearly confirmed that informed consents were obtained from all patients and healthy children. We had record and document participant consent in our hospital. And the ethics committees of our hospital had approved this consent procedure.

Plasma preparation, RNA isolation

Whole blood (2 mL) was collected from each subject, and plasma was separated at 1,600 g for 10 min by centrifugation at room temperature. Then removal of all cell debris was followed at 16,000 g for 10 min by centrifugation

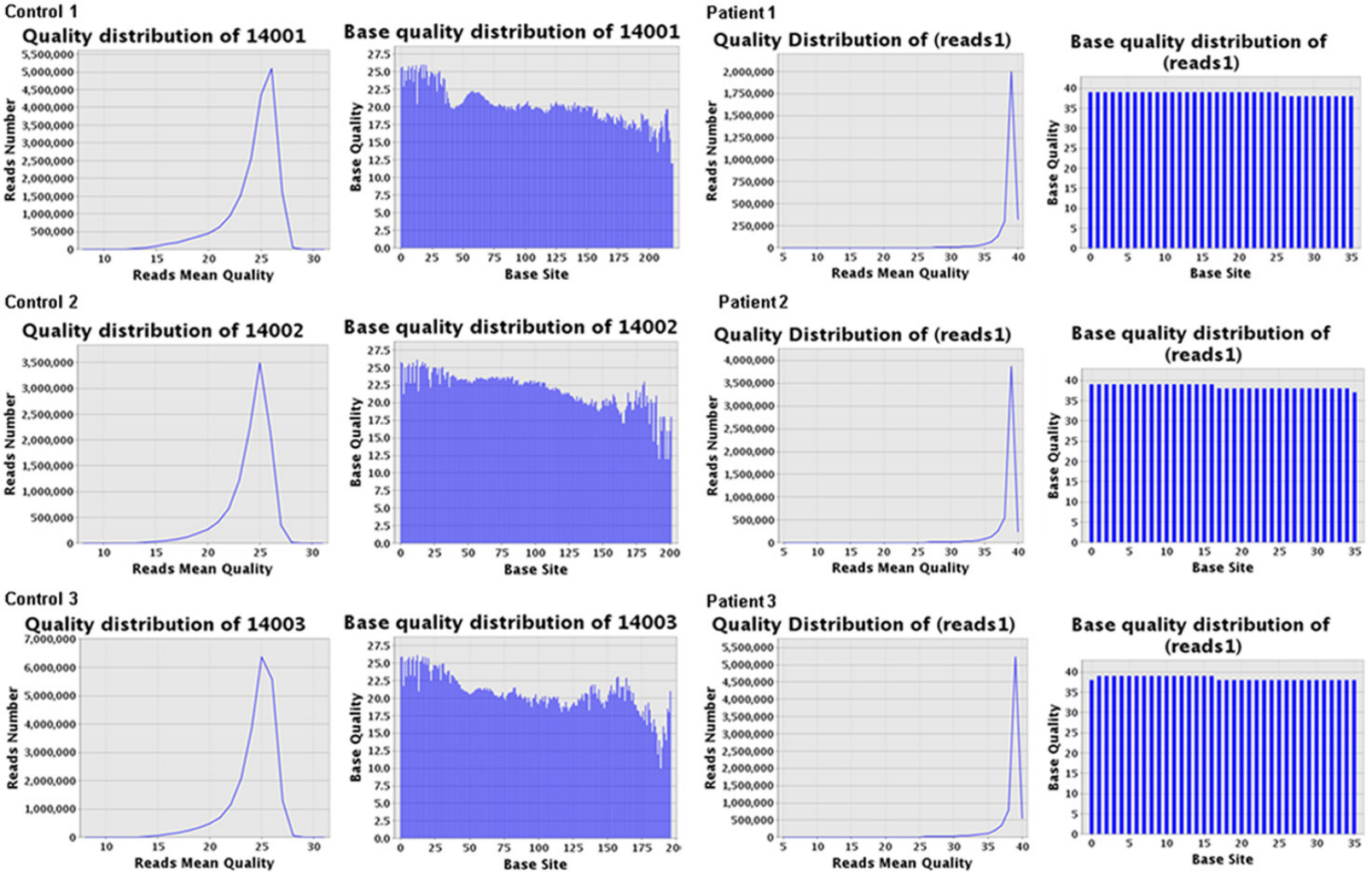
Control 1
Quality distribution of 14001
Reads Number
Reads Mean Quality
Base quality distribution of 14001
Base Quality
Base Site
Patient 1
Quality Distribution of (reads1)
Reads Number
Reads Mean Quality
Base quality distribution of (reads1)
Base Quality
Base Site
Control 2
Quality distribution of 14002
Reads Number
Reads Mean Quality
Base quality distribution of 14002
Base Quality
Base Site
Patient 2
Quality Distribution of (reads1)
Reads Number
Reads Mean Quality
Base quality distribution of (reads1)
Base Quality
Base Site
Control 3
Quality distribution of 14003
Reads Number
Reads Mean Quality
Base quality distribution of 14003
Base Quality
Base Site
Patient 3
Quality Distribution of (reads1)
Reads Number
Reads Mean Quality
Base quality distribution of (reads1)
Base Quality
Base Site

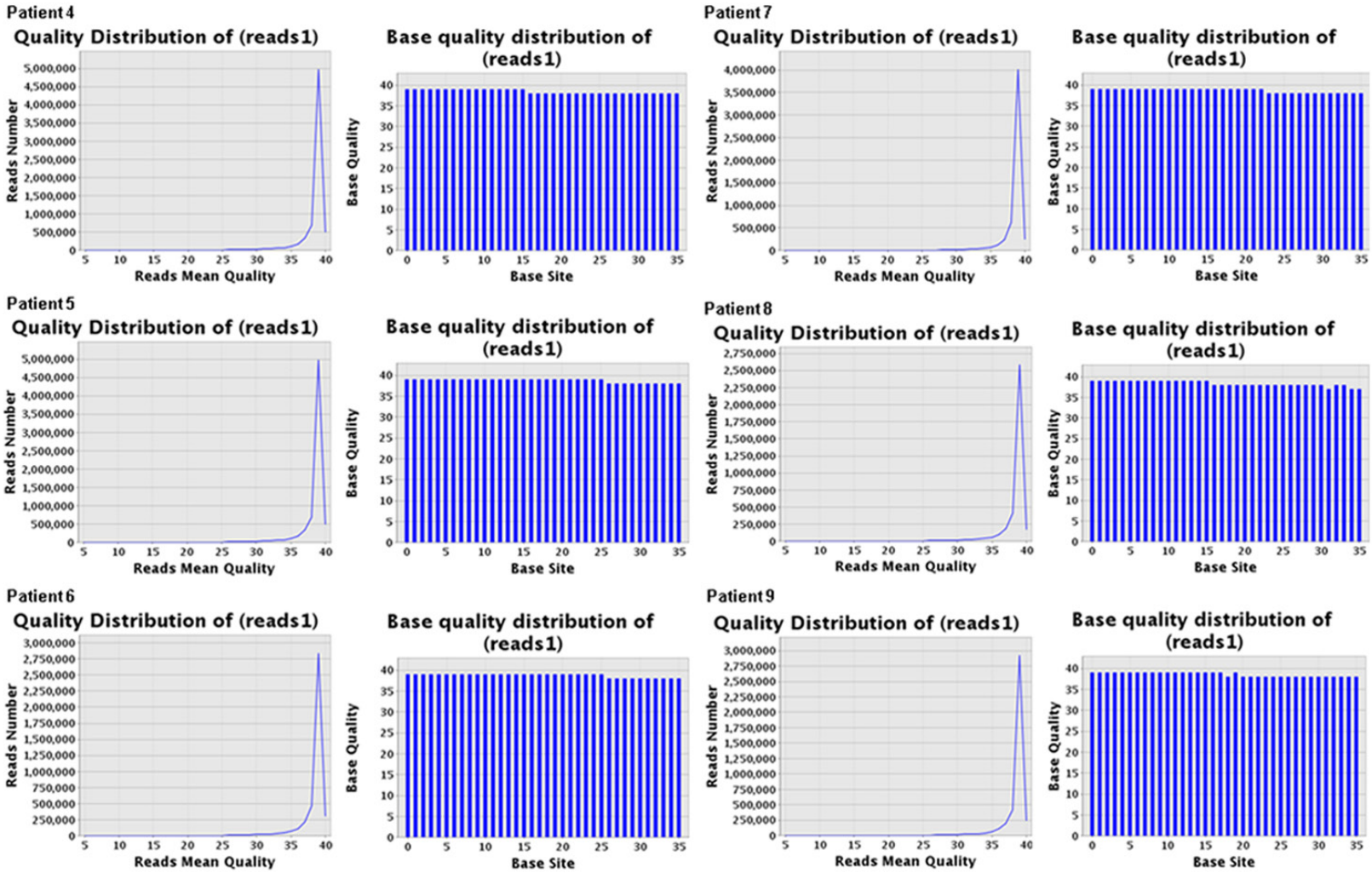

Figure 1. Quality of sequencing. According to the statistical results, the average quality of more than 99 percent of reads was larger than 20 in each sample.

Table 3. Data pre-processing of NGS

Sample	Trim 3' adapter (%)	Short reads
Control 1 (14001)	173,485 (0.9)	1,988,375 (10.8)
Control 2 (14002)	103,023 (0.9)	1,111,470 (9.8)
Control 3 (14003)	185,786 (0.8)	2,198,221 (9.7)
Patient 1 (XH)	4,171,652 (97.3)	2,763,371 (64.5)
Patient 2 (LXY)	5,069,495 (92.6)	2,342,920 (42.8)
Patient 3 (XMX)	5,438,345 (97.1)	2,552,773 (45.6)
Patient 4 (LZD)	7,713,565 (94.0)	3,350,342 (43.4)
Patient 5 (ZMY)	3,623,320 (96.4)	1,505,942 (40.0)
Patient 6 (MCW)	7,249,629 (97.8)	3,517,848 (48.5)
Patient 7 (ZWH)	3,956,990 (94.2)	1,996,908 (47.5)
Patient 8 (WYH)	5,563,679 (98.9)	4,481,675 (79.7)
Patient 9 (LTJ)	2,964,077 (98.3)	2,465,353 (81.8)

at 4°C. All the supernatant was collected to store at -80°C for further analysis.

RNA Extraction from plasma

Total RNA was extracted for the miRNA-sequencing test using TRIzol (Invitrogen, Carlsbad, CA, USA) and a miRNeasy Mini Kit (Qiagen, Valencia, CA, USA). And total RNA was harvested from 200-μl volumes of plasma for RT-qPCR assay by the mirVana™ PARIS™ Kit (Ambion, Foster City, CA, USA).

Next-generation sequencing

Hybridization and ligation were conducted for small RNA fraction not exceeding 50 nt using Adaptor Mix (*New England* Biolabs). Then RNAs were reversely transcribed followed by sequencing by microRNA sequencing with the Illumina HiSeq 2000 platform.

Data extraction and analysis

Data extraction and analysis was performed as showed in Flow Diagram 1. The sequences of all the mature miRNAs were identified together with 5 flanking nucleotides through the library preparation of reference sequences in miRBase version 19 [14]. Given that the length of minimum read were 50 nucleotides, specific adapters were used to anneal to their 3' ends and extended the entire small RNAs during the library preparation. Thus, we removed the adapters and obtained the potential miRNAs with the length of 15-30 nucleotides for further analysis using cut adapt software in silico [15]. Subsequently, the sequences were perfectly matched with the prepared reference library for using Bowtie v 0.12.7 [16]. Then we computed the numbers of mapped reads for every miRNA presented as two ways: (1) the number of each of the unique reads mapped to each reference sequence, and (2) the number of all total reads mapped to each reference sequence. Acquired data of all samples were normalized with the Reads per Million (RPM) normalization. According to the formula, RPM equal to (Nref/Nall)×10^6. Nref means the number of reads mapped to the miRNA reference, and Nall refers to total number of reads mapped in the sample [17].

Statistical analysis

Welch *t*-test-paired was performed for comparison of isomiRs deregulation and selection of miRNAs between patients and control samples. False discovery rate (FDR) was used to evaluate the errors due to multiple comparisons. On the basis of the expression profiles, Hierarchical clustering of selected miRNAs was conducted using Ward's agglomeration method. Target Rank software was performed to identify the significantly deregulated target genes of each miRNA seed sequence between patients and control samples [17, 18]. The volcano plot was used to further identify differential microRNAs expression between the two groups. Moreover, the cluster analysis was performed, and the spearman correlation coefficient was calculated and analyzed. Furthermore, the gene ontology (GO) consortium and data was used to analyze the targets gene of differential microRNAs.

Statistical differences between groups were analyzed with two-tailed paired Student *t*-test. Continuous variables with normally distributed were represented as SD (mean ± standard deviation). Abnormally distributed data between groups were analysis using Kruskal-Wallis ANOVA. All statistical analyses were performed with SPSS software version 18.0. $P<0.05$ was considered with statistically significant.

Results

Capacity and quality of sequencing

We obtained 18,395,453, 11,348,541 and 22,646,434 qualified Illumina reads from three healthy controls, or 4,287,101, 5,473,799,

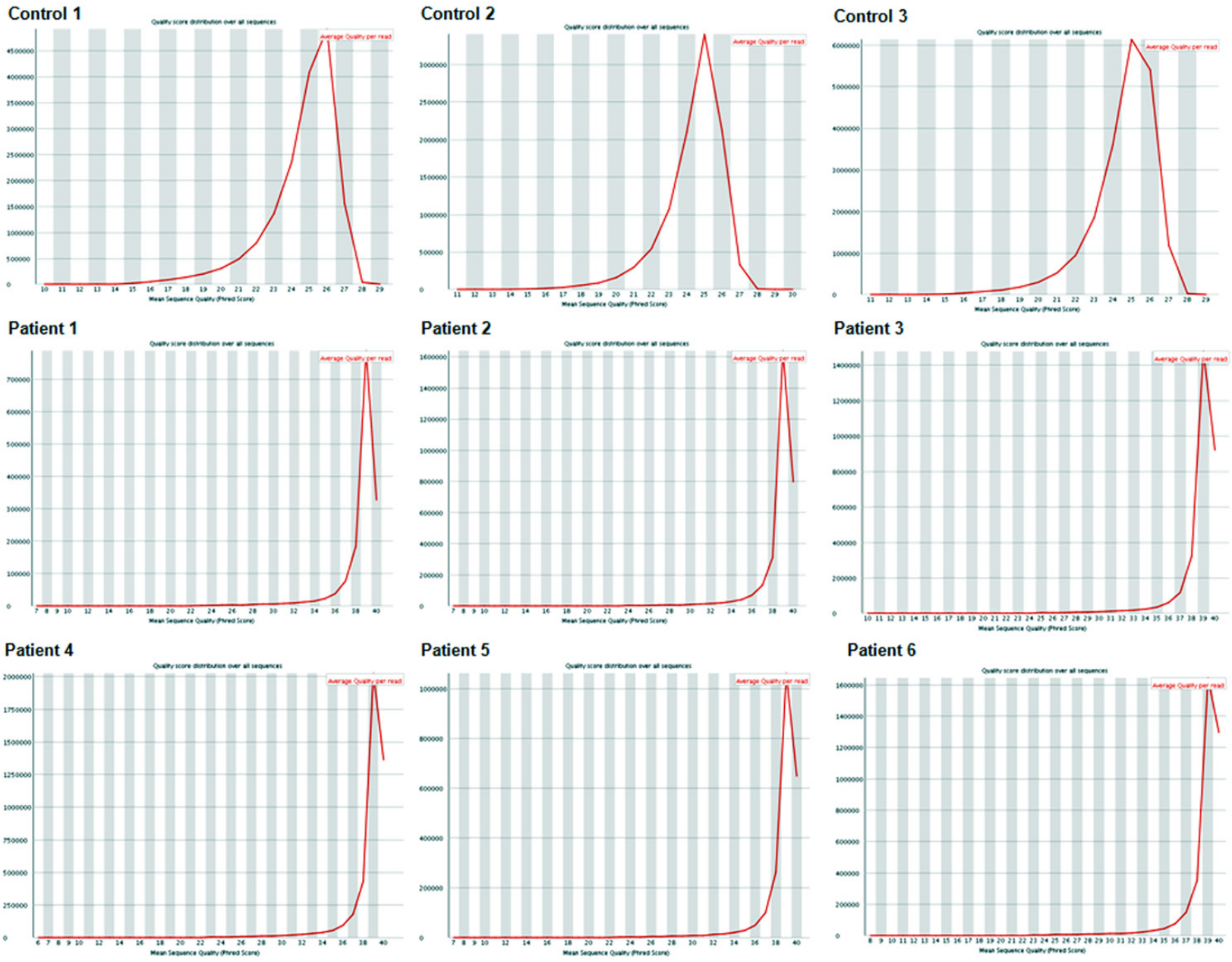
Control 1
Control 2
Control 3
Patient 1
Patient 2
Patient 3
Patient 4
Patient 5
Patient 6

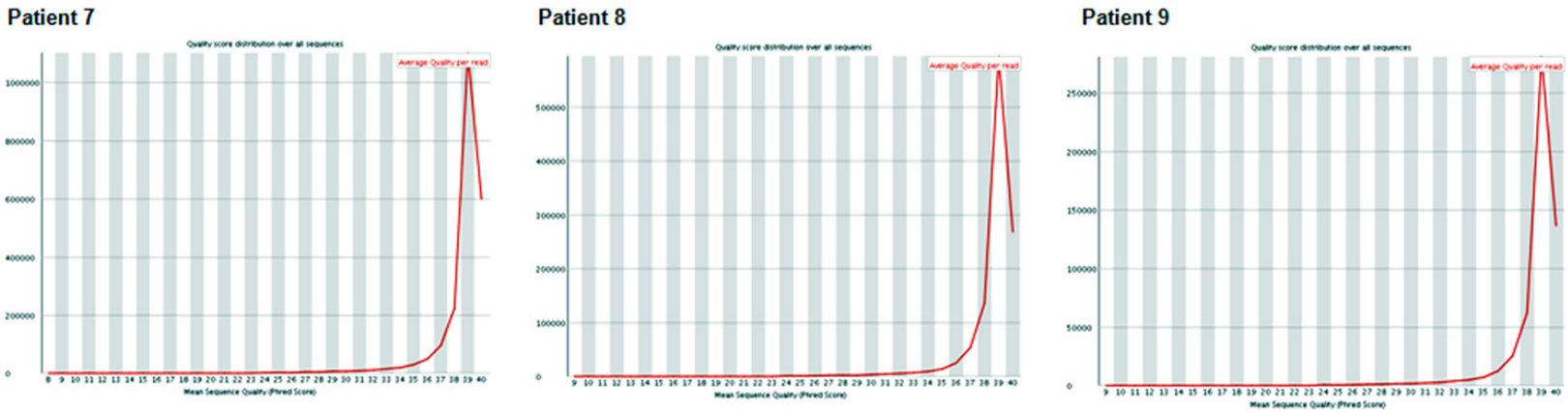

Figure 2. Per sequence quality scores. The low quality reads was removed by fastq_quality_filter program, so that the quality score of at least 95% base was not low than 20.

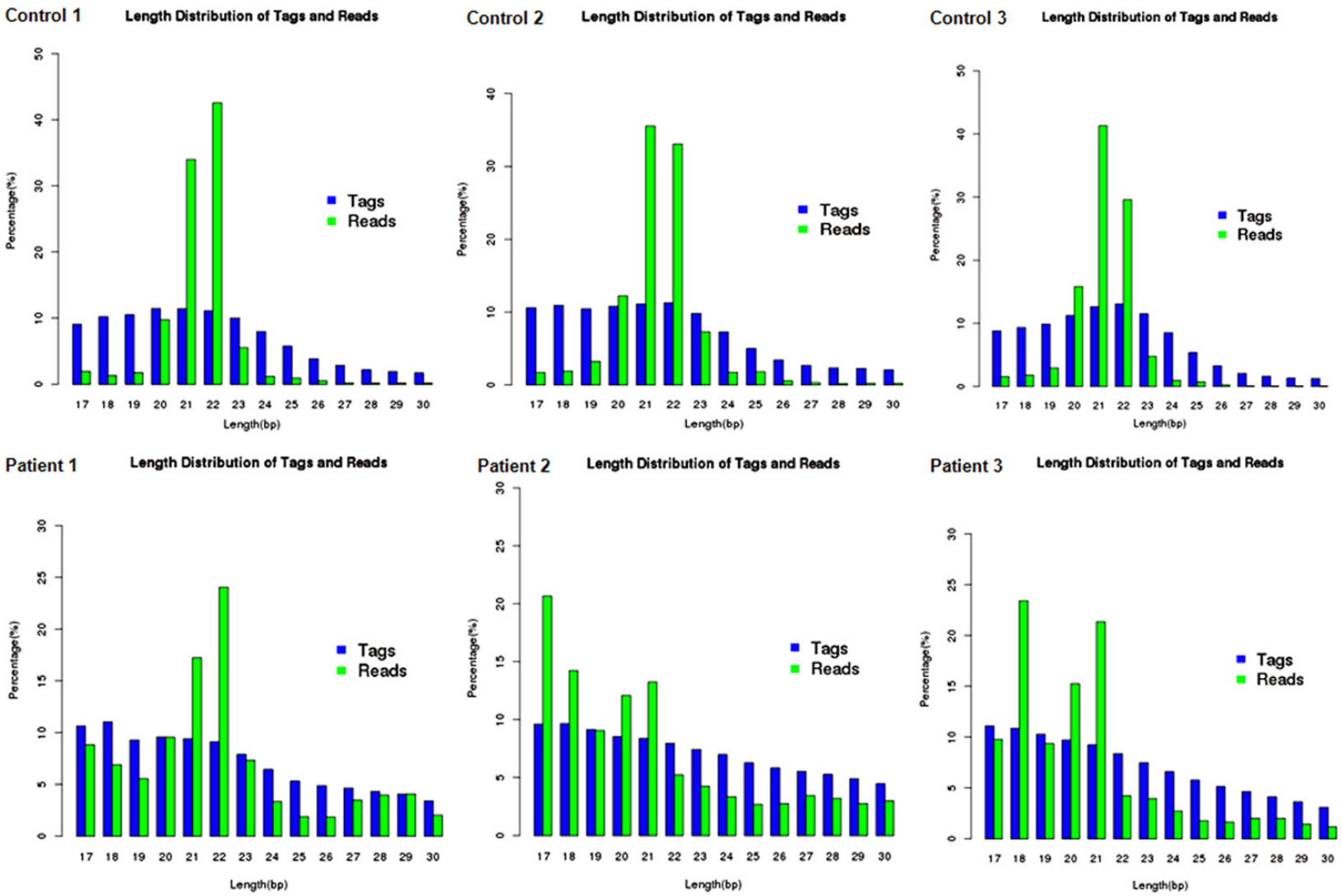
Control 1
Length Distribution of Tags and Reads
Control 2
Length Distribution of Tags and Reads
Control 3
Length Distribution of Tags and Reads
Patient 1
Length Distribution of Tags and Reads
Patient 2
Length Distribution of Tags and Reads
Patient 3
Length Distribution of Tags and Reads
Tags
Reads
Percentage(%)
Length(bp)
17 18 19 20 21 22 23 24 25 26 27 28 29 30

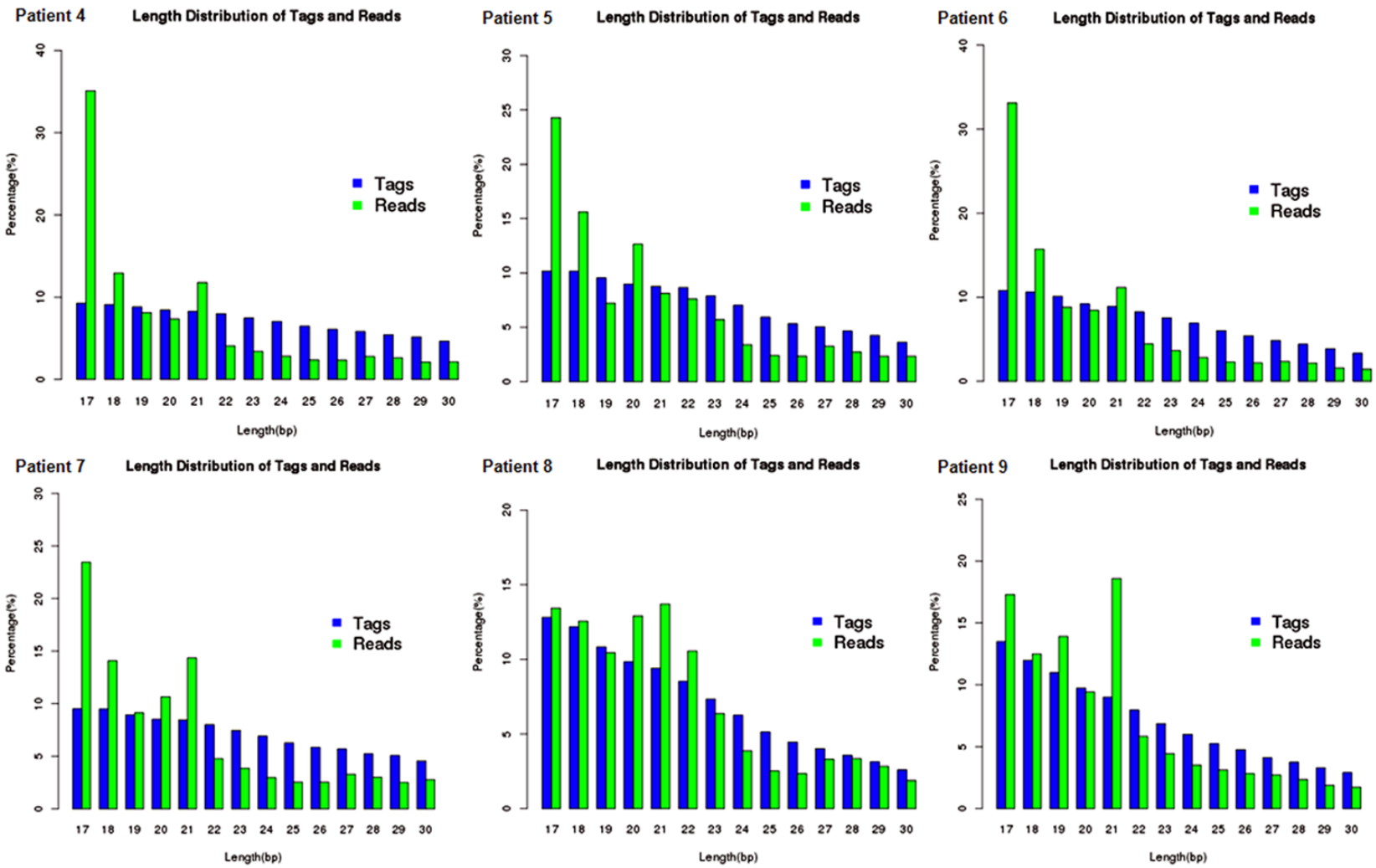

Figure 3. The length distribution of tags and reads. The length of mature microRNA sequence distributed range from 17-30 nt, then sequences in the range was analyzed. The length distribution of tags and reads were showed in above Figure.

Table 4. Genome mapped tags and reads

Sample	Processed Reads	Alignment ($1 \leq m^d \leq 5$)	Failed	Alignment suppressed ($m^d > 5$)
Control 1 (14001)	16,407,708	15,465,411 (94.26)	512,778 (3.13)	428,889 (2.61)
Control 2 (14002)	10,237,071	9,659,527 (94.36)	273,290 (2.67)	304,254 (2.97)
Control 3 (14003)	20,448,213	19,659,601 (96.14)	484,011 (2.37)	304,601 (1.49)
Patient 1 (XH)	1,523,730	1,061,412 (69.66)	276,465 (18.14)	185,853 (12.20)
Patient 2 (LXY)	3,130,879	2,054,697 (65.63)	368,730 (11.77)	707,182 (22.61)
Patient 3 (XMX)	3,045,532	2,229,938 (73.22)	414,763 (13.62)	400, 831 (13.16)
Patient 4 (LZD)	4,363,223	2,449,906 (56.15)	440,633 (10.10)	1,472,684 (33.75)
Patient 5 (ZMY)	2,260,972	1,455,027 (64.35)	242,198 (10.71)	563,747 (13.16)
Patient 6 (MCW)	3,731,781	2,042,342 (54.73)	337,887 (9.05)	1,351,552 (36.22)
Patient 7 (ZWH)	2,202,752	1,405,721 (63.82)	245,822 (11.16)	551,209 (25.02)
Patient 8 (WYH)	1,141,645	653,446 (57.24)	330,057 (28.91)	158,142 (13.85)
Patient 9 (LTJ)	549,312	256,496 (46.69)	200,642 (36.53)	92,174 (16.78)

Note: The bowtie parameter (-m=5, suppress all alignments if >5 exist); d, dap.

5,598,305, 7,713,565, 3,766,914, 7,249,629, 4,199,660, 5,623,320 and 3,014,665 qualified Illumina reads from nine pediatric patients, respectively (**Table 1**). The statistical analysis demonstrated that the average quality of every sample was larger than 20, and indicated that the quality was very fine (**Table 2** and **Figure 1**).

Data pre-processing of NGS

Firstly, the 3'-adapter sequence (AGATCGGAAGAGCACACGTCT) was identified from raw data of NGS (**Table 3**) by fastx_cliper program. Then we used fastq_quality_filter program to remove the reads of lower quality, so that the short reads was obtained (**Table 3**) and the quality score of at least 95% base was not low than 20 (**Figure 2**). Then the cluster was performed to mark all identical sequences as one tag. The results showed that the length of all the filtered mature microRNA sequences distributed range from 17-30 nt, and then sequences in the range was analyzed (**Figure 3**). The length distribution of tags and reads were showed in **Figure 3**.

Analysis of small RNA

All the marked tags were mapped onto sequence of *Homo sapiens* genome in PubMed, by the match software bowtie 0.12.7. **Table 4** displayed the mapped tags and reads computed on account of 17~30 nt reads or tags. **Figure 4** showed the genome-mapped rates of samples. Then we used the database Rfam 11.0 of RNA family to analyse sundry RNAs in the samples (**Table 5**).

Analysis of microRNA and different microRNAs between two groups

The Mirdeep (version 2) was utilized to forecast the microRNAs of the samples. The differential microRNAs were analyzed with edgeR software for differential expression analysis. Then the major different microRNAs between IgAN group and healthy control group were showed in **Table 6**. The volcano plot was used to further identify differential microRNAs expression between the two groups (**Figure 5**). Moreover, the cluster analysis was performed (**Figure 6**), and the spearman correlation coefficient was calculated and analyzed (**Figure 7**). Furthermore, the gene ontology (GO) consortium and data was used to analyze the targets gene of different microRNAs (**Figure 8**).

Discussion

The absolute quantification of next generation sequencing (NGS) is just modestly accurate. The advance of high-throughput sequencing was driven by the high demand of low-cost sequencing, which is known as NGS. Thousands of sequences concurrently manufactured in NGS process. In recent years, the computational analysis of genome-wide scale is increasingly functioned as a backbone to facilitate more novel biomedical discovery. However, owing to the exponential increase of the quantities of sequence data, the bottleneck analysis remains yet to be solved.

In this study, we performed a microRNA sequencing analysis of the plasma microRNAs

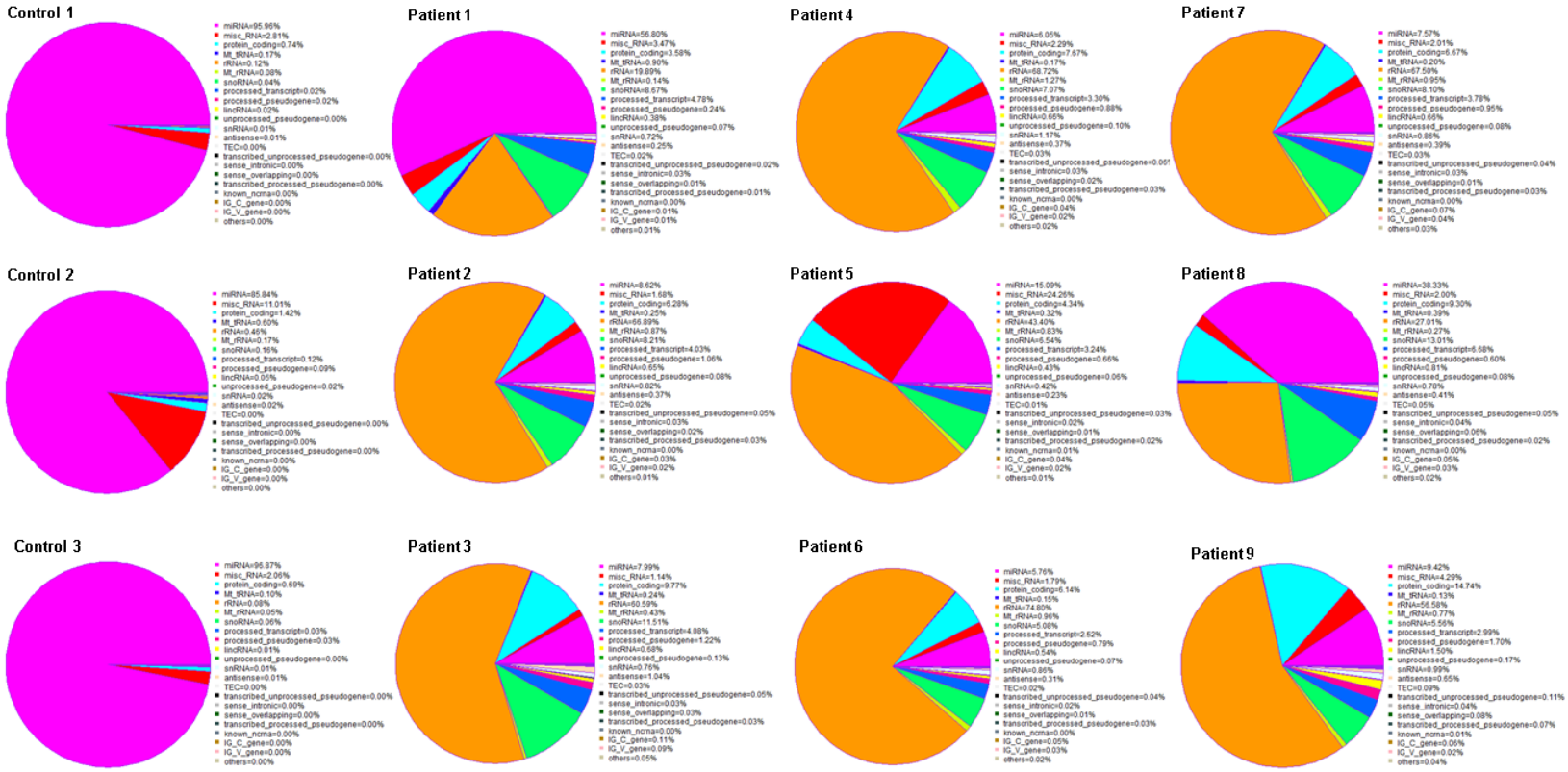

Figure 4. The sRNA length distribution. The tags were showed in Figure.

Table 5. The data of reads by Rfam analysis

	14001[a]	14002[a]	14003[a]	XH[b]	LTJ[b]	LXY[b]	LZD[b]	MCW[b]	WYH[b]	XMX[b]	ZMY[b]	ZWH[b]
MiRNA	14956240	4755406	13669396	579912	6931	77782	76903	72272	115245	38899	137407	50221
misc_RNA	437782	610205	290673	35382	3154	15126	29170	22500	6023	5558	220890	13303
Protein_coding	115670	78791	97140	36531	10850	56657	97571	77146	27970	47530	39535	44264
Mt_tRNA	25729	33405	14059	9148	92	2216	2223	1873	1164	1179	2925	1296
rRNA	18553	25450	11509	203083	41636	603626	874030	939094	81202	294841	395113	447690
Mt_rRNA	12091	9558	6586	1435	567	7832	16153	12048	806	2095	7552	6329
snoRNA	6384	8892	8103	88520	4091	74057	89938	63807	39126	56016	59551	53722
Processed_transcript	3173	6410	4072	48805	2199	36374	41951	31649	20100	19845	29489	25052
Processed_pseudogene	3070	5193	3745	2485	1250	9586	11155	9933	1800	5939	5998	6297
lincRNA	2391	2630	1936	3896	1107	5863	8388	6776	2448	3306	3934	4364
snRNA	1727	1065	1660	7313	725	7364	14921	10793	2352	3681	3816	5674
Antisense	1490	925	1284	2519	477	3320	4763	3860	1219	5042	2085	2581
Unprocessed_pseudogene	585	1122	498	722	123	722	1307	913	247	654	515	511
Transcribed_unprocessed_pseudogene	282	222	111	231	83	407	775	538	165	256	284	286
TEC	209	240	187	207	63	184	443	295	152	156	130	190
Sense_intronic	135	178	104	336	33	279	419	306	117	166	153	224
Sense_overlapping	106	83	117	103	56	175	196	169	172	127	85	84
Transcribed_processed_pseudogene	62	70	64	85	51	275	445	332	64	157	169	223
Unitary_pseudogene	15	10	11	39	15	22	39	37	18	29	9	11
Known_ncrna	10	21	4	23	6	28	61	26	1	0	47	19
IG_C_gene	4	20	5	92	44	252	567	610	144	554	396	461
IG_V_gene	0	14	0	53	18	148	282	336	100	416	171	239

a, control; b, patient.

Table 6. The different microRNAs between IgAN group and healthy control group

MiRNA	logFC	logCPM	*P* Value	FDR	Regulation
hsa-miR-16-5p	-9.673921	18.070719	1.41E-22	1.00E-19	Down
hsa-miR-17-5p	-9.054284	14.094769	8.69E-22	3.09E-19	Down
hsa-miR-18a-5p	-9.335749	12.228062	2.99E-18	7.10E-16	Down
hsa-miR-106b-5p	-7.166413	11.731259	8.54E-18	1.52E-15	Down
hsa-miR-15b-5p	-9.662802	13.729845	1.67E-17	2.38E-15	Down
hsa-miR-15a-5p	-9.14362	13.518393	4.58E-17	5.43E-15	Down
hsa-miR-20b-5p	-8.431402	11.24096	8.44E-17	8.59E-15	Down
hsa-miR-144-5p	-10.59912	13.966664	1.55E-15	1.38E-13	Down
hsa-miR-106a-5p	-6.068976	11.060429	3.79E-15	3.00E-13	Down
hsa-miR-19b-3p	-7.532036	13.087462	9.35E-15	6.05E-13	Down
hsa-miR-107	-6.44509	10.684797	8.87E-15	6.05E-13	Down
hsa-miR-93-5p	-7.056658	12.845438	2.17E-14	1.29E-12	Down
hsa-miR-451a	-8.997146	19.044948	2.40E-13	1.32E-11	Down
hsa-miR-15b-3p	-6.273676	9.0980813	9.01E-13	4.28E-11	Down
hsa-miR-20a-5p	-5.092674	13.274778	8.54E-13	4.28E-11	Down
hsa-miR-151a-5p	-5.059851	11.139807	1.24E-12	5.54E-11	Down
hsa-miR-130a-3p	-8.690139	9.9721012	1.71E-12	7.16E-11	Down
hsa-miR-223-3p	-8.59944	14.569363	3.49E-12	1.38E-10	Down
hsa-miR-19a-3p	-7.41424	11.058379	4.47E-12	1.61E-10	Down
hsa-miR-1291	8.516153	9.3103726	4.53E-12	1.61E-10	Up

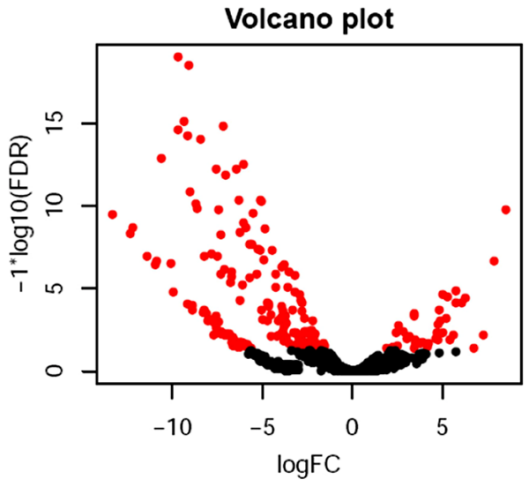

Figure 5. The volcano plot. The volcano plot was used to further identify differential microRNAs expression between the two groups.

in pediatric patient with IgA nephropathy or health control by NGS, using the Illumina Deep Sequencing technology. We obtained 18,395,453, 11,348,541 and 22,646,434 qualified Illumina reads from three healthy controls, and 4,287,101, 5,473,799, 5,598,305, 7,713,565, 3,766,914, 7,249,629, 4,199,660, 5,623,320 and 3,014,665 qualified Illumina reads from nine pediatric patients, respectively. The average quality of more than 99 percent of reads was larger than 20, indicative of good quality of these data. Then we used the fastx cliper program to perform data pre-processing of NGS, and removed the lower quality reads using fastq quality filter program. Subsequently, cluster was carried out; the distribution of the length of mature microRNAs sequence ranged from 18-30 nt and mapped onto the sequence of *Homo sapiens* genome. Then we used the Miranda software to predict the target genes of microRNAs (score >150, energy <-15).

Rfam is a database of RNA families, and known as a collection of multiple sequence alignments and covariance models. It is available on the US and the UK website. These websites can enable the users to probe a query sequence against the library of covariance models, and to browse family annotation and multiple sequence alignments. The users could download the database in flat file form and search locally by the INFERNAL package (http://infernal.wustl.edu/).

Comparative microRNAs analysis revealed those 2591 microRNAs differentially between pediatric patients and healthy controls, including one expression of microRNA was up-regulated and 19 expression of microRNAs were down-regulated. The volcano plot was used to further identify differential microRNAs expression between the two groups. Moreover, the cluster analysis was performed, and the spearman correlation coefficient was calculated and analyzed. Furthermore, the gene ontology (GO) consortium and data was used to analyze the targets gene of differential microRNAs.

The edgeR software, an achievement of methology designed by Smyth and Robinson [20, 21], is a bio-conductor package for analysing differ-

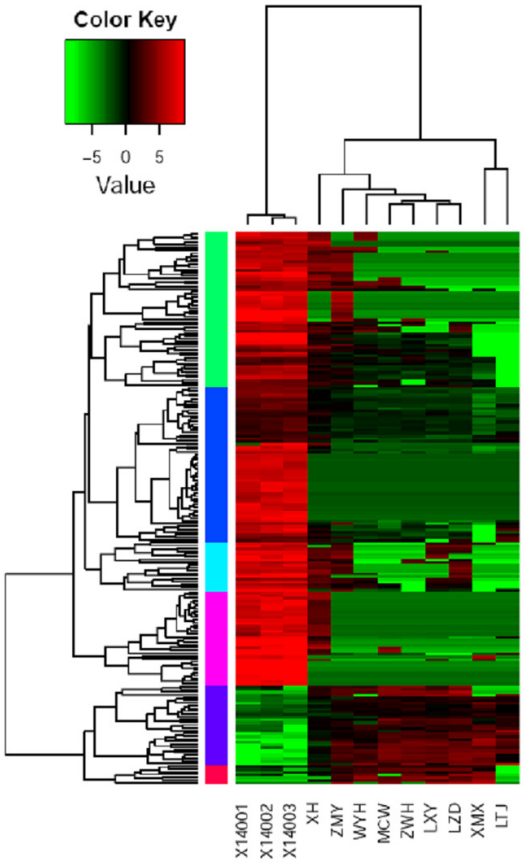

Figure 6. The cluster analysis. The cluster analysis was performed.

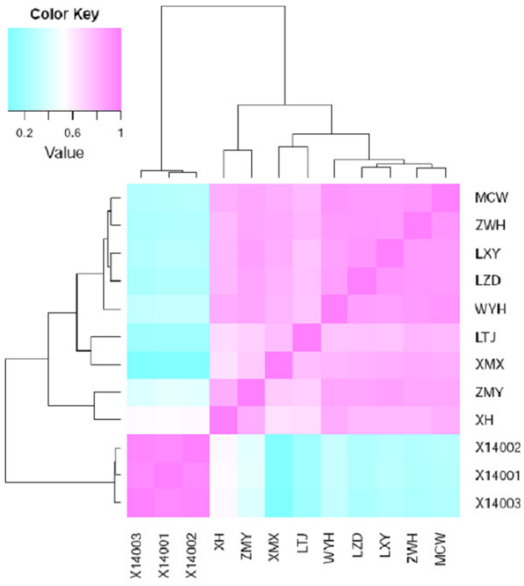

Figure 7. The spearman correlation cofficient. The spearman correlation coefficient was calculated and analyzed.

ential gene expression [19]. The software and methods can also be applied to emerging technologies like RNA-seq [22, 23] to obtain digital expression data. Statistically, a volcano plot can quickly examine differences in large datasets consisted of replicate data [24]. It displays fold-change and significance on the x- and y-axes, respectively. It can combine a measurement of statistical significance from a statistical test (e.g., a *p*-value of ANOVA test) with the magnitude of the change enabling quick visual identification of those data-points (genes, etc.) that display statistically significant large-magnitude changes.

MicroRNAs are a classification of short, non-coding RNAs, which can modulate the expression of target protein-coding genes through binding to 3', un-translated regions [25, 26]. Abnormal expression of microRNAs can give rise to aberrant expression of target gene mRNAs. The expression of numerous genes could be regulated by a single miRNA [27], and a few of miRNAs might jointly modulate the expression of only one gene with pivotal functions in a given tissue [28]. The microRNA can recognize target mRNA depending on the specific region of a miRNA that comprises 2-8 nucleotides of mature molecule.

Plenty of studies about miRNA aberrances primarily focused on the analysis of canonical, reference miRNAs, while isomiRs required more advanced technologies, like NGS and laborious analysis of all the acquired data. Hence, our study employed NGS to acquire microRNA data come from between pediatric patients and healthy controls by next generation sequencing techniques. Numbers of microRNAs will be pivotal for revealing the molecular regulatory mechanisms of expression relevant to the pathogenesis and pathophysiology of IgAN.

That the miRNAs groups expressed distinguishingly in blood, kidney and urine demonstrate that they are tissue-specific. *In silico* analysis has shown that a miRNA may monitor their expression of numerous target genes; this means miRNAs may have an important role in biological regulation. Studies in the present study suggest that various miRNAs might have specific roles in IgAN. In some limited conditions, miRNAs may be used as candidate biomarkers for early diagnosis of disease. Early

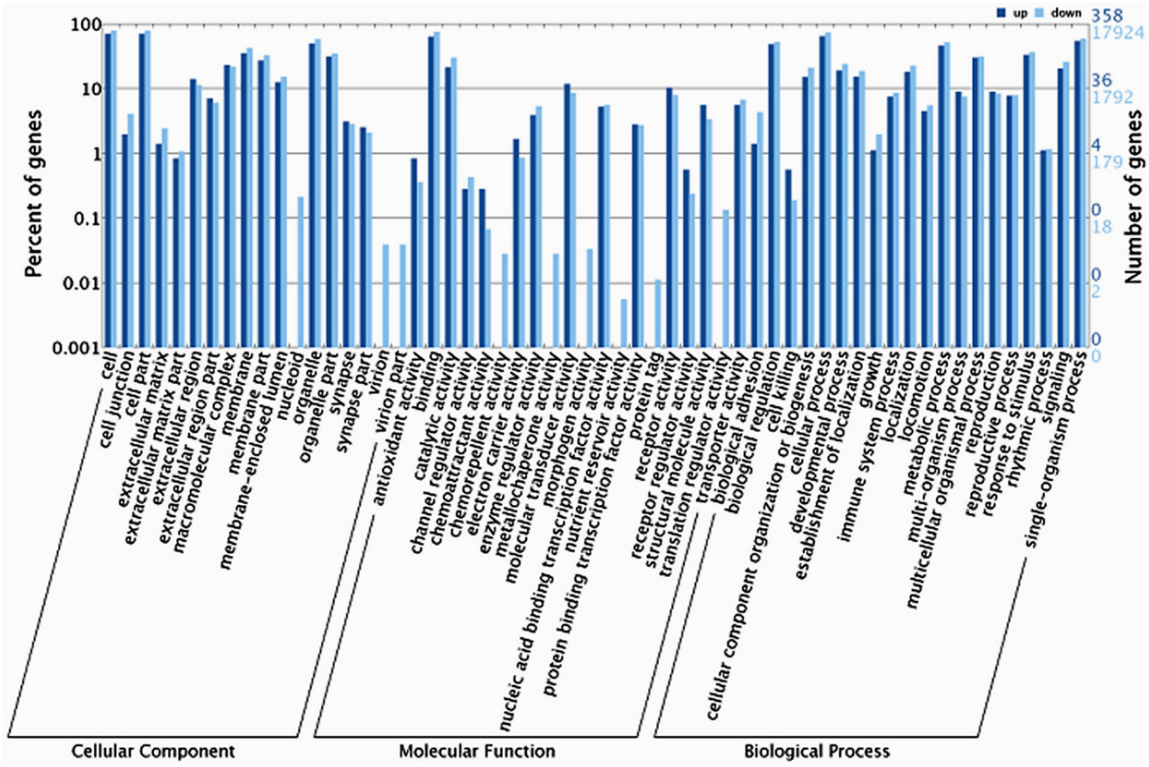

Figure 8. The gene ontology (GO) consortium and data. The gene ontology (GO) consortium and data was used to analyze the targets gene of different microRNAs.

detection of these miRNAs can intensify clinical management, promote long-term outcomes and highly improve the quality of life.

Limitations

The major limitation was the small samples on account of the complicated technical and expensive costs, which might introduce certain bias. Later, the expression levels of microRNAs will be detected between patient groups and control groups basing on our results in this investigation.

Acknowledgements

This work was supported by grants from Beijing Municipal Administration of Hospitals Youth Programme (QML20151102), and the National Natural Science Foundation of China (No. 81600551, No. 81070565).

Disclosure of conflict of interest

None.

Address correspondence to: Dr. Ying Shen, Department of Nephrology, Beijing Children's Hospital, Capital Medical University and Beijing Key Laboratory of Pediatric Chronic Kidney Disease and Blood Purification, No. 56, Nanlishi Road, West District, Beijing 100045, China. Tel: 86-10-59616161; 86-10-59616161; E-mail: ying_116sh@sohu.com

References

[1] Hartono C and Muthukumar T. Treating IgA nephropathy: quid novi? Discov Med 2014; 17: 131-138.

[2] D'Amico G. Natural history of idiopathic IgA nephropathy: role of clinical and histological prognostic factors. Am J Kidney Dis 2010; 36: 227-237.

[3] Moriyama T, Tanaka K, Iwasaki C, Oshima Y, Ochi A, Kataoka H, Itabashi M, Takei T, Uchida K and Nitta K. Prognosis in IgA nephropathy: 30-year analysis of 1,012 patients at a single center in Japan. PLoS One 2014; 9: e91756.

[4] Bellur SS, Troyanov S, Cook HT and Roberts IS. Immunostaining findings in IgA nephropathy: correlation with histology and clinical outcome in the Oxford classification patient cohort. Nephrol Dial Transplant 2011; 26: 2533-2536.

[5] Holley CL and Topkara VK. An introduction to small non-codingRNAs: miRNA and snoRNA. Cardiovas Drugs Therapy 2011; 25: 151-159.
[6] Bartel DP. MicroRNAs: Target Recognition and Regulatory Functions. Cell 2009; 136: 215-233.
[7] Arroyo JD, Chevillet JR, Kroh EM, Ruf IK, Pritchard CC, Gibson DF, Mitchell PS, Bennett CF, Pogosova-Agadjanyan EL, Stirewalt DL, Tait JF and Tewari M. Argonaute2 complexes carry a population of circulating microRNAs independent of vesicles in human plasma. Proc Natl Acad Sci U S A 2011; 108: 5003-5008.
[8] Li JY, Yong TY, Michael MZ and Gleadle JM. The role of microRNAs in kidney disease. Nephrology 2010; 15: 599-608.
[9] Bhatt K, Mi QS and Dong Z. MicroRNAs in kidneys: biogenesis, regulation, and pathophysiological roles. Am J Physiol Renal Physiol 2011; 300: F602-F610.
[10] Ho J and Kreidberg JA. The long and short of microRNAs in the kidney. J Am Soc Nephrol 2012; 23: 400-404
[11] Khella HW, Bakhet M, Lichner Z, Romaschin AD, Jewett MA and Yousef GM. MicroRNAs in kidney disease: an emerging understanding. Am J Kidney Dis 2013; 61: 798-808
[12] Sun Y, Koo S, White N, Peralta E, Esau C, Dean NM and Perera RJ. Development of a microarray to detect human and mouse microRNAs and characterization of expression in human organs. Nucleic Acids Res 2004; 32: e188.
[13] Tian Z, Greene AS, Pietrusz JL, Matus IR and Liang M. MicroRNA-target pairs in the rat kidney identified by microRNA microarray, proteomic, and bioinformatic analysis. Genome Res 2008; 18: 404-411.
[14] Kozomara A and Griffiths-Jones S. miRBase: integrating microRNA annotation anddeep-sequencing data. Nucleic Acids Res 2011; 39: D152-157.
[15] Martin MM. Cutadapt removes adaptor sequences from high-throughput sequenc-ing reads. EMBnetjournal 2011; 17: 10-12.
[16] Langmead B, Trapnell C, Pop M and Salzberg SL. Ultrafast and memory-efficient align-ment of short DNA sequences to the human genome. Genome Biol 2009; 10: R25.
[17] Wojcicka A, Swierniak M, Kornasiewicz O, Gierlikowski W, Maciag M, Kolanowska M, Kotlarek M, Gornicka B, Koperski L, Niewinski G, Krawczyk M and Jazdzewski K. Next generation sequencing reveals microRNA isoforms in livercirrhosis and hepatocellular carcinoma. Int J Biochem Cell Biol 2014; 53: 208-217.
[18] Nielsen CB, Shomron N, Sandberg R, Hornstein E, Kitzman J and Burge CB. Determi-nants of targeting by endogenous and exogenous microRNAs and siRNAs. RNA 2007; 13: 1894-1910.
[19] Robinson MD, McCarthy DJ and Smyth GK. edgeR: a Bioconductor package for differential expression analysis of digital gene expression data. Bioinformatics 2010; 26: 139-140.
[20] Robinson MD and Smyth GK. Moderated statistical tests for assessing differences in tag abundance. Bioinformatics 2007; 23: 2881-2887.
[21] Robinson MD and Smyth GK. Small-sample estimation of negative binomial dispersion, with applications to SAGE data. Biostatistics 2008; 9: 321-332.
[22] Li H, Lovci MT, Kwon YS, Rosenfeld MG, Fu XD and Yeo GW. Determination of tag density required for digital transcriptome analysis: application to an androgen-sensitive prostate cancer model. Proc Natl Acad Sci U S A 2008; 105: 20179-20184.
[23] Marioni JC, Mason CE, Mane SM, Stephens M and Gilad Y. RNA-seq: an assessment of technical reproducibility and comparison with gene expression arrays. Genome Res 2008; 18: 1509-1517.
[24] Cui X and Churchill GA. Statistical tests for differential expression in cDNA microarray experiments. Genome Biol 2003; 4: 210.
[25] Bartel DP. MicroRNAs: Target Recognition and Regulatory Functions. Cell 2009; 136: 215-233.
[26] Filipowicz W, Bhattacharyya SN and Sonenberg N. Mechanisms of post-transcriptionalregulation by microRNAs: are the answers in sight? Nat Rev Genet 2008; 9: 102-114.
[27] Lim LP, Lau NC, Garrett-Engele P, Grimson A, Schelter JM, Castle J, Bartel DP, Linsley PS and Johnson JM. Microarray analysis shows that some microRNAs downregulate large numbers of target mRNAs. Nature 2005; 433: 769.
[28] Jazdzewski K, Boguslawska J, Jendrzejewski J, Liyanarachchi S, Pachucki J, WardynKA, Nauman A and de la Chapelle A. Thyroid hormone receptor beta (THRB) is a major target gene for microRNAs deregulated in papillary thyroid carcinoma (PTC). J Clin Endocrinol Metab 2011; 96: E546-553.

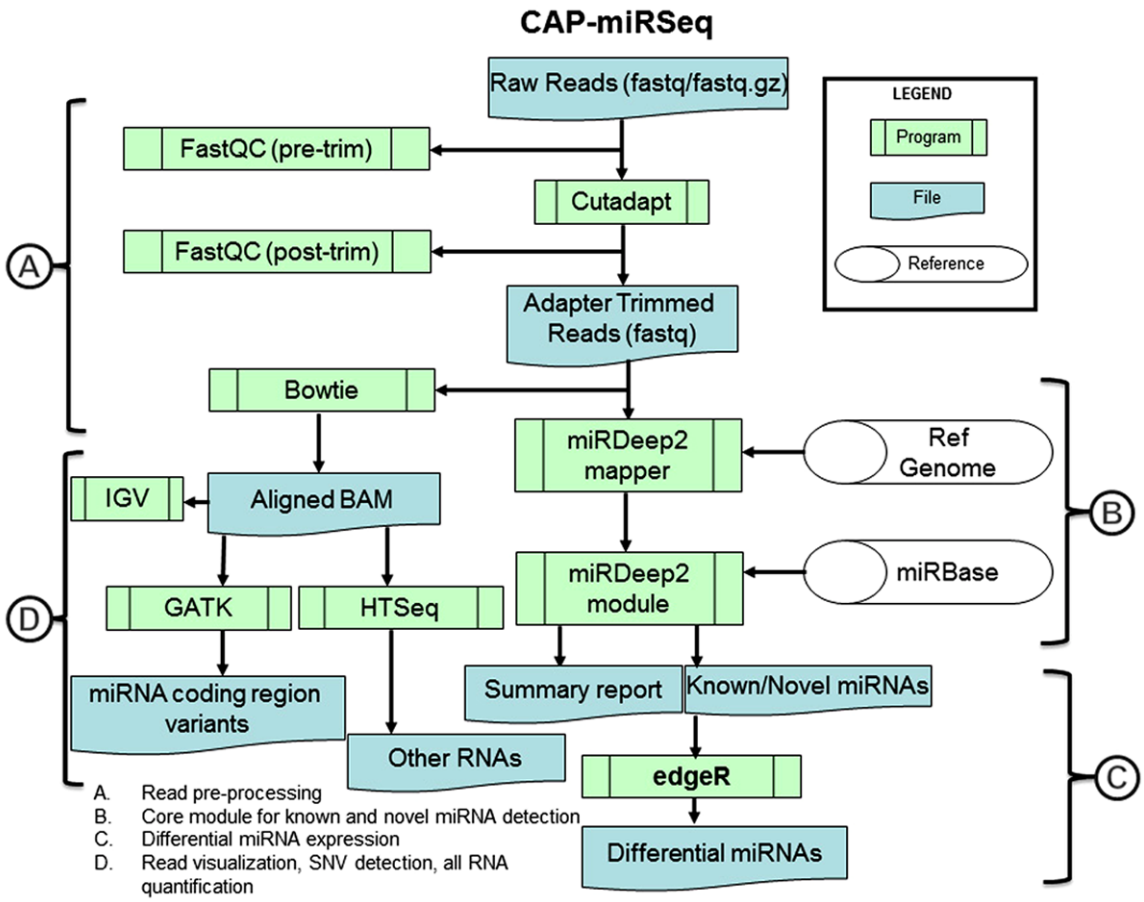

Flow Diagram 1. The process of sequence and data analysis.